THE JOURNAL OF BIOLOGICAL CHEMISTRY
Vol. 275, No. 51, Issue of December 22, pp. 39846–39854, 2000

Printed in U.S.A.

Modulation of L-type Ca^{2+} Channels by G$\beta\gamma$ and Calmodulin via Interactions with N and C Termini of α_{1C}*

Received for publication, July 5, 2000, and in revised form, August 28, 2000
Published, JBC Papers in Press, September 19, 2000, DOI 10.1074/jbc.M005881200

Tatiana Ivanina‡, Yakov Blumenstein‡, Elena Shistik, Rachel Barzilai, and Nathan Dascal§

From the Department of Physiology and Pharmacology, Sackler School of Medicine, Tel Aviv University, Ramat Aviv 69978, Israel

Neuronal voltage-dependent Ca^{2+} channels of the N (α_{1B}) and P/Q (α_{1A}) type are inhibited by neurotransmitters that activate $G_{i/o}$ G proteins; a major part of the inhibition is voltage-dependent, relieved by depolarization, and results from a direct binding of G$\beta\gamma$ subunit of G proteins to the channel. Since cardiac and neuronal L-type (α_{1C}) voltage-dependent Ca^{2+} channels are not modulated in this way, they are presumed to lack interaction with G$\beta\gamma$. However, here we demonstrate that both G$\beta\gamma$ and calmodulin directly bind to cytosolic N and C termini of the α_{1C} subunit. Coexpression of G$\beta\gamma$ reduces the current via the L-type channels. The inhibition depends on the presence of calmodulin, occurs at basal cellular levels of Ca^{2+}, and is eliminated by EGTA. The N and C termini of α_{1C} appear to serve as partially independent but interacting inhibitory gates. Deletion of the N terminus or of the distal half of the C terminus eliminates the inhibitory effect of G$\beta\gamma$. Deletion of the N terminus profoundly impairs the Ca^{2+}/calmodulin-dependent inactivation. We propose that G$\beta\gamma$ and calmodulin regulate the L-type Ca^{2+} channel in a concerted manner via a molecular inhibitory scaffold formed by N and C termini of α_{1C}.

Voltage-dependent Ca^{2+} channels (VDCCs)[1] are crucial for neuronal and muscular excitability (1). Mammalian VDCCs fall into several families distinguished by pharmacological and biophysical properties (L, N, P/Q, T, and R type) and the molecular identity of the main, pore−forming subunit, α_1 (2–4). The neuronal N- and P/Q-type channels, based on α_{1B} and α_{1A}, respectively, are crucial for neurotransmitter release (3). L-type Ca^{2+} channels containing the "cardiac-type" α_{1C} subunit regulate contraction of cardiac and smooth muscle, and excitability and gene expression in the brain (2, 5, 6). The α_1 subunits contain four homologous membrane domains numbered I−IV and 5 large intracellular segments: N terminus (NT), C terminus (CT), and linkers between the domains (often called loops L_1, L_2, and L_3). There is also a large number of short intracellular linkers between transmembrane segments within each domain.

Activation in all voltage-dependent channels is initiated by a voltage-driven shift in charged transmembrane elements (7). Nevertheless, the parts of the channel and the auxiliary subunits which are not exposed to the membrane electrical field may substantially modulate the gating (for reviews related to Ca^{2+} channels, see Ref. 3). In particular, VDCCs are strongly and specifically modulated by neurotransmitters acting via heterotrimeric G proteins, via actions on the cytosolic parts of the channel. Some of the modulations are mediated by G protein-triggered second messenger cascades, often via protein kinases A and C (PKA and PKC, respectively), others by a direct interaction with G protein subunits (1, 8–14). Both PKC and PKA alter VDCC gating parameters acting via cytosolic parts of α_1 or via the ancillary β subunit (15–19).

Neuronal VDCCs are usually inhibited by G protein-coupled receptors by *voltage-independent* (mediated by several second messenger pathways (20–23)) and *voltage-dependent* mechanisms. The latter is fast, membrane−delimited, mediated by G$\beta\gamma$, and occurs in α_{1A} (P/Q), α_{1B} (N), and α_{1E} (11–13). A hallmark of this modulation is relief of inhibition and acceleration of current activation by depolarization (*voltage-dependent facilitation*), which reflects a decrease in the affinity of the channel to G$\beta\gamma$ (24, 25). In α_{1A}, α_{1B}, and α_{1E} G$\beta\gamma$ binds to L_1 loop (15, 26, 27) and CT (27); NT is also important for the effect of G$\beta\gamma$, although a direct interaction has not yet been established (28–30). The relative functional roles of the L_1, CT-, and NT-binding sites are still unclear (27, 31, 32).

Cytosolic parts of α_1 subunits are also involved in inactivation gating. A major part of inactivation of L-type VDCCs is triggered by the entry of Ca^{2+} (33). Calmodulin (CaM) has been recently identified as the Ca^{2+} sensor indispensable for the Ca^{2+}-dependent inactivation in L (α_{1C})- and P/Q (α_{1A})-type channels (34–37). A CaM-binding site has been identified in the CT of α_{1C} and α_{1A}. Ca^{2+}-dependent CaM interaction with this domain has been found crucial not only for the Ca^{2+}-dependent inactivation, but also for an opposite effect of Ca^{2+}, called *Ca^{2+}-dependent facilitation* (34–37).

Despite the outstanding role of cytosolic segments in channel modulation, our ideas of how these parts affect the gating of the VDCCs are vague. The L-type (α_{1C}) channel is the best studied in this respect; but even here, only the roles of N and C termini have been examined. Removal of the distal half of the CT increases L-type channel currents and open probability by improving the coupling between gating charge (voltage sensor) movement and pore opening (38). It has been proposed that the CT acts as an inhibitory gate that conformationally restrains the opening of the channel (38, 39). Similarly to the CT, removal of the NT also enhances the open probability and the macroscopic currents in L-type channels, and a similar role (of an inhibitory gate) for the NT has been proposed (16, 17).

* This work was supported by National Institutes of Health Grant RO1 56260, Israel Science Foundation Grant 47/00, and the Tel Aviv University Research Fund. The costs of publication of this article were defrayed in part by the payment of page charges. This article must therefore be hereby marked "*advertisement*" in accordance with 18 U.S.C. Section 1734 solely to indicate this fact.

‡ Contributed equally to the results of this report.

§ To whom correspondence should be addressed. Tel:. 972-3-6409863; Fax: 972-3-6409113; E-mail: dascaln@post.tau.ac.il.

[1] The abbreviations used are: VDCC, voltage-dependent calcium channel; CaM, calmodulin; CT, C terminus; NT, N terminus; PKA, protein kinase A; PKC, protein kinase C; GST, glutathione *S*-transferase; aa, amino acid(s); Tricine, *N*-[2-hydroxy-1,1-bis(hydroxymethyl) ethyl]glycine; BAPTA, 1,2-bis(*O*-aminophenoxy)ethane-*N,N,N′,N′*-tetraacetic acid.

The L-type channel is not inhibited by neurotransmitters in a voltage-dependent manner (32, 40–42), and the L_1 loop of α_{1C} does not bind G$\beta\gamma$ (15, 26, 27). Voltage-dependent facilitation has been demonstrated in L-type VDCC, but it was PKA- rather than G protein-dependent (Refs. 40 and 43; however, see Ref. 44). Therefore, α_{1C} has been assumed to lack any interaction with G$\beta\gamma$. α_{1C} even served in several studies as a donor of presumably G$\beta\gamma$-indifferent parts, to create chimeras with other α_1 types, in the search for parts of α_1 that determine the sensitivity to G$\beta\gamma$. However, here we demonstrate that G$\beta\gamma$ binds to NT and CT of α_{1C} and inhibits the L-type VDCC in a voltage-independent but calmodulin-dependent manner. We identify a novel CaM-binding site in the NT, which, like the previously identified CT-binding site, is an important determinant of the Ca^{2+}/CaM-dependent inactivation. We propose a model in which NT and CT of the L-type channel form a scaffold that plays a role of an inhibitory gate which integrates the regulatory effects of G$\beta\gamma$ and CaM.

EXPERIMENTAL PROCEDURES

cDNA Constructs and mRNA—The cDNAs of the G protein subunits (bovine Gβ_1, bovine Gβ_2, human Gβ_3, mouse Gβ_4 and bovine Gγ_2; provided by M. Simon, Caltech) were either amplified by polymerase chain reaction to create *Eco*RI sites at the 5′ and 3′ ends (Gβ_1 and Gγ_2) or excised with *Eco*RI from the original vectors (all the others) and then subcloned into the *Eco*RI site of the pGEMHE (Gβ_1, Gβ_2, and Gγ_2) and pGEMHJ (Gβ_3 and Gβ_4) vectors (45, 46). The cDNAs of CaM and CaM_{1234} (47) were provided by J. P. Adelman. cDNAs and RNAs of rabbit Ca^{2+} channels subunits β_2A and α_2/δ were as described (48). The rabbit heart α_{1C} cDNA (49) and all its mutants used here were subcloned into *Sal*I/*Hin*dIII sites of the pGEM-SB vector (16). The N-terminal deletion mutant of α_{1C}, ΔN_{2-139}, was prepared as described (16). To create the α_{1C} C-terminal truncation mutant $\Delta C_{1700\text{-end}}$, polymerase chain reaction amplification of a C-terminal part of α_{1C} was performed to create a stop codon after nucleotide 5274 (numbering by Ref. 49) followed by a *Hin*dIII site. The truncated cDNA was subcloned back into pGEM-SB. The ΔNΔC mutant was constructed by cutting and ligating the appropriate parts of ΔN_{2-139} and $\Delta C_{1700\text{-end}}$ mutants. The RNAs were prepared using a standard procedure (50).

cDNAs designed to create glutathione *S*-transferase (GST) fusion proteins were constructed using polymerase chain reaction strategy, with primers containing the desired restriction sites and linked in-frame to GST, as described (16). The cDNA constructs encoded the GST fusion proteins of the following segments of α_{1C}: whole N terminus (N_{1-154}); CT and three C-terminal cDNA fragments (C, aa 1505–2171; C_0, aa 1505–1846; C_1, aa 1664–1845; and C2, aa 1841–2171); L_1, aa 438–550; L_2, aa 783–930; and L_3, aa 1196–1249.

Oocytes and Electrophysiology—Xenopus laevis frogs were maintained and dissected as described (50). Oocytes were injected with equal amounts (by weight) of the mRNAs of α_{1C} or its mutants with of α_2/δ, with or without β_2A, and incubated for 3–5 days at 20–22 °C in NDE96 solution (96 mM NaCl, 2 mM KCl, 1 mM $MgCl_2$, 1 mM $CaCl_2$, 2.5 mM Na pyruvate, 50 μg/ml gentamycine, 5 mM HEPES, pH 7.5). Whole cell currents were recorded using the Gene Clamp 500 amplifier (Axon Instruments, Foster City, CA) using the two-electrode voltage clamp technique in a solution containing 40 mM $Ba(OH)_2$ or 40 mM $Ca(OH)_2$, 50 mM NaOH, 2 mM KOH, and 5 mM HEPES, titrated to pH 7.5 with methanesulfonic acid. In some cases, a solution with 2 mM Ba^{2+} was used (2 mM $Ba(OH)_2$, 96 mM NaOH, 2 mM KOH, 5 mM Hepes, pH titrated to 7.5 with methanesulfonic acid). Stimulation, data acquisition, and analysis were performed using pCLAMP software (Axon Instruments). Ba^{2+} currents were measured by a 200 or 400 ms step to 20 mV from a holding potential of −80 mV.

Interaction between GST Fusion Proteins and in Vitro Synthesized $G_{\beta\gamma}$ and Calmodulin—The procedures were essentially as described (16). In brief, [^{35}S]Met/Cys-labeled Gβ_1, Gγ_2, CaM, and CaM_{1234} were translated on the template of *in vitro* synthesized RNAs using a rabbit reticulocyte translation kit (Promega). The fusion proteins were synthesized and extracted from *Escherichia coli* using the Amersham Pharmacia Biotech kit. Purified GST fusion proteins (5–10 μg) or purified GST (10 μg) were incubated with 5 μl of the lysate, containing the ^{35}S-labeled proteins in 500 μl of phosphate-buffered saline with 0.05% Tween 20, for 2 h at room temperature, with gentle rocking. In some experiments the incubation was done in the presence of 1 mM $CaCl_2$ or 5 mM EGTA. In the experiments shown in Fig. 5*C*, the incubation was done in the same buffer but with varying concentrations of free Ca^{2+}, in the presence of 2 mM EGTA; free Ca^{2+} concentration was calculated using the MAXC program. Then 30 μl of glutathione-Sepharose beads (Amersham Pharmacia Biotech) were added, and the mixture was incubated for 30 min at 4 °C and washed four times in 1 ml of the same buffer. Following washing, GST fusion proteins were eluted with 30 μl of 20 mM reduced glutathione in elution buffer (120 mM NaCl, 100 mM Tris-HCl, pH 8). CaM was analyzed on 15%, Gβ, on 12% SDS-polyacrylamide gels. Gγ was analyzed on Tricine ready-made gels (Bio-Rad). The labeled products were identified and quantified by autoradiography using a PhosphorImager (Molecular Dynamics) as described (51). Phosphorylation of the N-terminal GST fusion protein was performed as described (17).

Immunochemistry of the Expressed α_{1C} in Xenopus Oocytes—This was performed essentially as described (51, 52). Oocytes were injected with mRNAs and incubated in NDE solution containing 0.5 mCi/ml [^{35}S]methionine/cysteine (Amersham Pharmacia Biotech) for 4 days at 22 °C. Plasma membranes were separated manually (51) from the rest of the oocyte (designated as internal fraction). 10–20 membranes and 3–5 internal fractions, or 5 whole oocytes, were homogenized, proteins were solubilized, immunoprecipitated as described (16, 52), and electrophoresed on 6 or 3–8% polyacrylamide-SDS gels. Card-I antibody was kindly provided by M. M. Hosey (Northwestern University, Chicago) (53).

Presentation and Analysis of the Experimental Results—The data are presented as mean ± S.E. To overcome the problem of batch-to-batch variability in current amplitudes, the results were normalized as follows (54): in each oocyte, I_{Ba} was normalized to the mean amplitude of I_{Ba} in the control group of oocytes of the same donor. These normalized values were averaged across all oocyte batches tested. Comparisons between two groups (*e.g.* control and G$\beta\gamma$-expressing groups) were tested for statistically significant differences ($p < 0.05$ or better) using two-tailed unpaired *t* tests. Comparison between several groups was done using one-way analysis of variance (ANOVA) followed by Dunnet's or Tukey's tests, using the SigmaStat software (SPSS Corp.).

RESULTS

G$\beta\gamma$ Binds to Intracellular Segments of α_{1C}—Direct interaction between intracellular segments of α_{1C} with G$\beta\gamma$ was studied *in vitro* using fragments of α_{1C} fused to GST, covering all the large intracellular segments of α_{1C} (Fig. 1*A*). They included the whole NT (N_{1-154}), the full-length CT (C), three subdivisions of the C terminus (C_0, C_1, and C_2, as shown in Fig. 1*A*, *inset*), and three interdomain linker loops (L_1, L_2, and L_3). The binding of G$\beta\gamma$ to NT, CT, or its parts, and L_3 has not been examined in the past. The GST fusion proteins were immobilized on glutathione-agarose beads and assayed for interaction with *in vitro* translated, ^{35}S-labeled G$\beta_1\gamma_2$ subunits. Unexpectedly, NT and CT bound G$\beta_1\gamma_2$, whereas GST alone and loops L_1, L_2, and L_3 did not bind G$\beta\gamma$ (Fig. 1*B, upper panel*). The results of all experiments were quantitated by normalizing the ^{35}S-G$\beta\gamma$ signal obtained from each GST fusion protein to that of the NT obtained in the same experiment (Fig. 1*B, lower panel*). The CT exhibited the strongest interaction with G$\beta\gamma$, mainly localized to its proximal half (C_0; aa residues 1505–1846). The distal half of the CT, C_2, showed a weak but reproducible G$\beta\gamma$ binding. Since there is no binding in the middle of CT (C_1), it is plausible that G$\beta\gamma$ binds to two separate sites in the CT, roughly in its first quarter (from the beginning of C_0 to the beginning of C_1, between aa 1505 and 1664) and the last half. NT showed intermediate G$\beta\gamma$ binding. Fig. 1*C* shows that the binding of G$\beta\gamma$ to NT and CT was Ca^{2+}-independent: it was identical in the presence of 1 mM Ca^{2+} or 5 mM EGTA, or with no additions (control). The binding of G$\beta\gamma$ to NT (which is a PKC substrate: see Ref. 17) was not affected by phosphorylation by PKC or by the presence of the Ca^{2+} channel β_2A subunit (data not shown).

Of the 5 known Gβ proteins (55), the highly homologous Gβ_1 through Gβ_4 often show considerable selectivity in modulating the voltage-dependent Ca^{2+} channels (Refs. 56–58; but see Ref. 59). However, in α_{1C}, all four β subunits (presented, in all cases, with Gγ_2) bound well to NT and CT (Fig. 1*D*). Gβ could

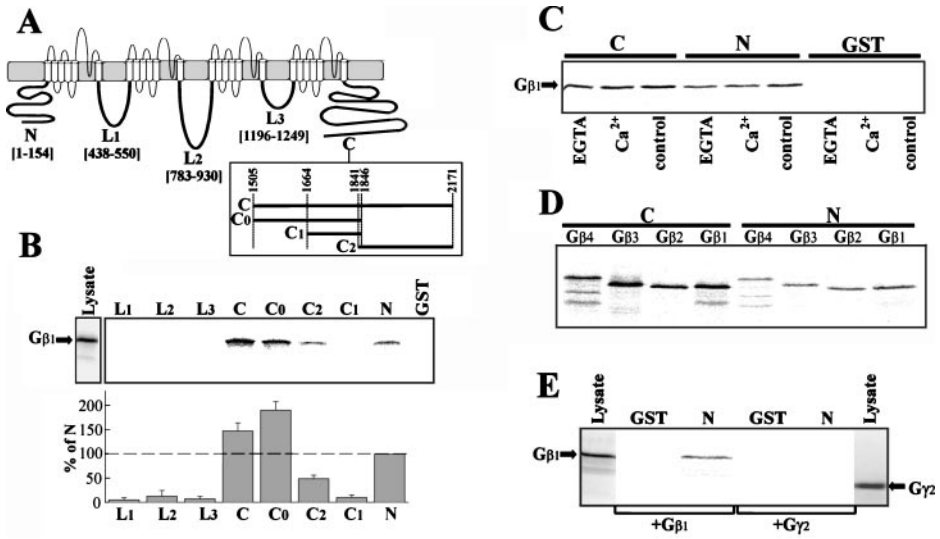

FIG. 1. **Interaction of G$\beta\gamma$ with GST fusion proteins encompassing fragments of the α_{1C} subunit of L-type Ca^{2+} channel.** *A,* schematic presentation of the α_{1C} subunit. The intracellular segments of α_{1C}, corresponding to the GST fusion proteins used in this study, are shown in *bold*. The *inset* shows the subdivision of the C terminus according to the four GST fusion proteins used. *B,* interaction between GST-fused fragments of α_{1C} subunit of L-type Ca^{2+} channel and ^{35}S-radiolabeled *in vitro* translated $G\beta_1\gamma_2$, demonstrated by the detection of ^{35}S-labeled $G\beta_1$ on the radiogram. The *upper panel* shows a representative experiment, done in the absence of added Ca^{2+} or EGTA. The plot on the *lower panel* shows the summary of 7–13 experiments in which the binding of $G\beta_1\gamma_2$ to the various channel fragments has been compared. In each experiment, the intensity of the signal given by each fragment was normalized to that produced by G$\beta\gamma$ bound to the N terminus (which was present in all experiments). The lane showing the signal obtained from the labeled protein synthesized in the reticulocyte lysate ("lysate") was loaded with 1 μl of lysate, whereas 5 μl were added to each reaction with GST fusion proteins. *C,* the binding of G$\beta\gamma$ to N and C termini of α_{1C} is Ca^{2+}-independent. There is no difference in the level of G$\beta\gamma$ binding in control conditions (when no additions to the reaction mixture have been made) and in the presence of 1 mM Ca^{2+} or 5 mM EGTA. *D,* binding of $G\beta_1\gamma_2$, $G\beta_2\gamma_2$, $G\beta_3\gamma_2$, and $G\beta_4\gamma_2$ to the NT and CT of α_{1C}. *E*, the presence of the γ subunit is not necessary for the binding of $G\beta_1$ to the N terminus. $G\beta_1$ and $G\gamma_2$ were synthesized *in vitro* separately and their interaction with the GST-fused N terminus was tested, also separately, by the standard procedure. The eluates of the two reactions were run on the same gel. $G\beta_1$, but not $G\gamma_2$, was found to bind to the N terminus.

bind to NT of α_{1C} without the Gγ, while $G\gamma_2$ did not bind (Fig. 1*E*), as also has been shown for L_1 of α_{1B} (58).

Coexpression of G$\beta\gamma$ Attenuates the L-type Ca^{2+} Channel Currents—Although L-type Ca^{2+} currents in neurons are down-regulated by activation of $G_{i/o}$-coupled neurotransmitter receptors (see "Discussion"), such modulations could not be reproduced in two expression systems, oocytes and HEK cells (31, 32, 40–42). It seemed the G$\beta\gamma$, when released from G proteins after activation of the relevant neurotransmitters by agonists, did not directly regulate the L-type channel. This leaves open the question of the functional consequences of the interaction between α_{1C} and G$\beta\gamma$ revealed by experiments of Fig. 1. To address this problem, we used coexpression methodology. L-type channels were expressed in *Xenopus* oocytes in full subunit composition (α_{1C}, $\alpha_2\delta$ and β_2A), or without the β subunit ($\alpha_1\alpha_2\delta$ combination). Currents were measured using the two-electrode voltage clamp technique. At standard levels of expression of the channel used here (1 ng of RNA/oocyte for $\alpha_1\alpha_2\delta\beta$, 2.5 ng/oocyte for $\alpha_1\alpha_2\delta$), the average I_{Ba} was 1064 ± 47 nA (n = 58 oocytes, N = 8 batches) and 324 ± 15 nA (n = 149, N = 19), respectively.

In accord with previous reports, activation by acetylcholine of a coexpressed muscarinic m2 receptor (which couples to $G_{i/o}$ proteins) did not cause any consistent modulation of I_{Ba} (data not shown). However, upon additional coexpression of $G\alpha_o$, which is indispensable for muscarinic inhibition of L-type Ca^{2+} channels in pituitary neurons (60), acetylcholine caused a substantial inhibition of I_{Ba} in 2 out of 5 oocyte batches tested (data not shown). The inconsistency of modulation suggests that additional unidentified proteins (lacking in some oocyte batches) are important for the effect of acetylcholine.

In contrast, coexpression of $G\beta_1\gamma_2$ reproducibly decreased I_{Ba} by ~40% in all oocyte batches tested (Fig. 2, *A* and *C*). In each batch, currents were normalized to the average I_{Ba} in control group; this allowed the comparison and quantitation of effects of G$\beta\gamma$ coexpression in many batches. At standard levels of channel expression, the current decrease caused by the coexpression of G$\beta\gamma$ in the full subunit combination was 39.4 ± 2.7% (n = 58 oocytes from 8 batches), and in $\alpha_1\alpha_2\delta$ combination the decrease was 38.6 ± 2% (n = 149 oocytes from 19 batches; Fig. 2*C*). The inhibitory effect of coexpressed G$\beta\gamma$ on I_{Ba} was suppressed by coexpression of G$\beta\gamma$ scavengers: free $G\alpha_{i1}$ and the myristoylated C-terminal fragment of GIRK1 K^+ channel, $GIRK_{183-501}$src (61) (data not shown). The inhibition by G$\beta\gamma$ was clearly dose-dependent; a maximal inhibition was observed already at 0.5–1 ng/oocyte Gβ RNA (0.1–0.2 ng/oocyte Gγ RNA), and half-maximal effective doses were 0.17 and 0.07 ng/oocyte Gβ RNA for the full and $\alpha_1\alpha_2\delta$ subunit combinations, respectively (Fig. 2*B*). In all following experiments, Gβ and Gγ RNAs were always injected at supramaximal doses, 5 and 1 ng/oocyte, respectively.

We noticed that the inhibitory effect of G$\beta\gamma$ coexpression became smaller when more channels were expressed. This was investigated with $\alpha_1\alpha_2\delta$ channels expressed in increasing amounts by injecting 1.25, 2.5, or 5 ng/oocyte of each subunits RNA (Fig. 2*C*). At the highest concentration of channel RNA, the inhibition was lost and even replaced by a small but statistically significant 17 ± 5% enhancement (Fig. 2*C, right panel*). The same trend was observed in the channels of full subunit combination (Fig. 2*C, left panel*). G$\beta\gamma$ containing any of the four Gβ subunits tested in Fig. 1, $G\beta_1$ through $G\beta_4$, inhibited I_{Ba} approximately to the same extent as $G\beta_1$ with the standard RNA concentrations (Fig. 2*D*).

To exclude the possibility of a G$\beta\gamma$ effect on the level of Ca^{2+} channel expression, in two separate oocyte batches the RNA of $G\beta_1\gamma_2$ was injected 4 days after the injection of RNAs of α_1 and $\alpha_2\delta$, and I_{Ba} was measured 3 days later. (I_{Ba} reaches a steady level 3–4 days after RNA expression; data not shown.) In these experiments, the decrease in I_{Ba} was 35.5 ± 3.7% (n = 16, N = 2).

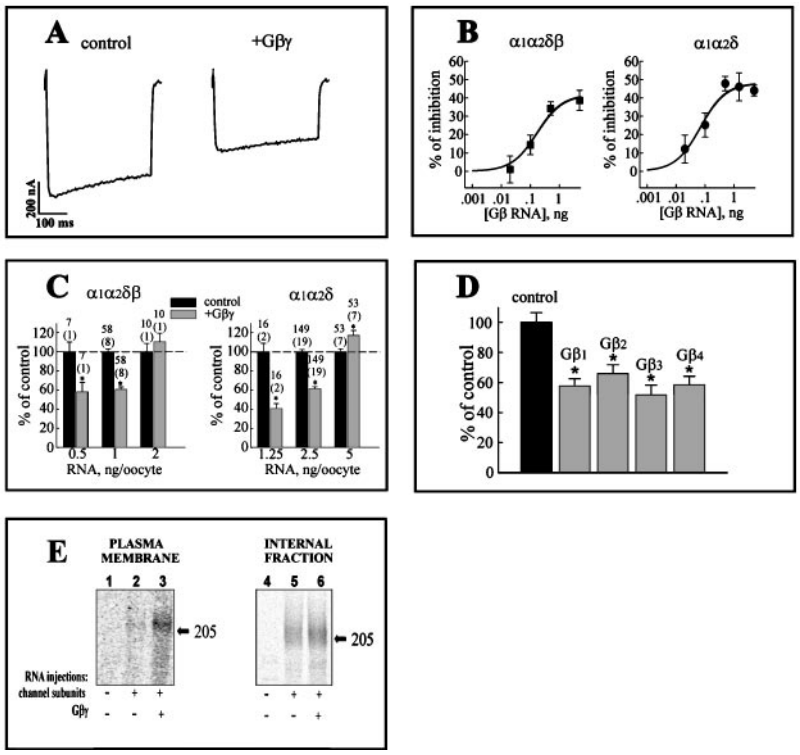

FIG. 2. **Coexpression of G$\beta\gamma$ modulates L-type channel currents.** Effects of G$\beta\gamma$ (5 ng of Gβ RNA and 1 ng of Gγ RNA per oocyte) coexpressed with different amounts of Ca^{2+} channels. RNAs of Gβ and Gγ were injected simultaneously with the RNAs of channel subunits. Ca^{2+} channel currents were measured with 40 mM Ba^{2+} as the charge carrier. *A,* representative Ba^{2+} currents in control (no G$\beta\gamma$) and G$\beta\gamma$-injected oocytes of one batch, measured by voltage steps from −80 to +20 mV**,** in channels of full subunit combination (α_{1C} + $\alpha_2\delta$ + β_2A; 1 ng of each subunits RNA per oocyte). *B,* G$\beta\gamma$-induced inhibition as a function of level of expression of G$\beta\gamma$. The RNAs of G$\beta\gamma$ and the channel subunits were injected simultaneously. The amounts of channel subunits RNAs were: 1 ng/oocyte in the full subunit composition, 2.5 ng in the $\alpha_1\alpha_2\delta$ composition. The amount of injected Gγ RNA was always one-fifth of that of Gβ. *C,* G$\beta\gamma$-induced inhibition of I_{Ba} is attenuated at high levels of channel expression. Data were normalized as described under "Experimental Procedures." *Asterisks* (*) indicate statistically significant differences ($p <$ 0.05 or better) between the control and G$\beta\gamma$-expressing groups. *Numbers above bars* indicate the number of cells assayed, *numbers* in *parentheses* indicate the number of oocyte batches. *D,* coexpression of all four Gβ subunits (with Gγ_2) inhibits I_{Ba}. Same conditions as in *A*. Each *bar* represents mean ± S.E. from 15 oocytes of one batch. *, $p < 0.05$ by two-way ANOVA followed by Dunnet test. *E,* coexpression of $G_{\beta\gamma}$ does not decrease the level of α_{1C} protein in the oocyte. The channels were expressed as $\alpha_1\alpha_2\delta$ (2.5 ng of RNA), with or without G$\beta\gamma$, labeled *in vivo* with [^{35}S]methionine/cysteine, and immunoprecipitated from 10 plasma membranes and 3 internal fractions after a 4-day incubation. Because of the low amount of α_{1C} protein in the plasma membrane, longer exposure of the gel to PhosphorImager cassette was used for the plasma membrane than for the internal fraction.

The effect of coexpression of G$\beta\gamma$ on the total level of expression of α_{1C} protein was further studied by quantitative immunoprecipitation of ^{35}S-labeled α_{1C} from *in vitro* metabolically labeled oocytes. α_{1C} was immunoprecipitated from manually separated plasma membranes and from the rest of the oocytes ("internal fraction") as described (51). Previously, we used 5 ng of RNA/oocyte to visualize α_{1C} in plasma membranes (16). This time, to assure that these biochemical measurements are compatible with the electrophysiological ones described above, we used the standard RNA doses (2.5 ng/oocyte; $\alpha_1\alpha_2\delta$ subunit combination). Despite the low level of α_1C protein expression in the plasma membrane obtained under these conditions, it was clear that the amount of α_{1C} in the plasma membrane was rather increased by coexpression of G$\beta\gamma$ (Fig. 2*E, left panel*). Similarly, a slight increase of the amount of immunoprecipitated α_{1C} was observed in the internal fraction containing the cytosol and the intracellular membranes (Fig. 2*E, right panel*). Similar results were obtained in two additional experiments with 2.5 ng of RNA/oocyte, and with higher levels of subunit expression (5 ng of RNA/oocyte; data not shown). Thus, G$\beta\gamma$-induced inhibition does not correlate with changes in the amount of α_{1C} protein in plasma membrane; it is due to an effect on channels gating. Since the inhibition is lost at high levels of channel expression, we hypothesized that this effect of G$\beta\gamma$ depends on the presence of a factor which is in short supply in oocytes.

Roles of N and C Termini in Gating and in Mediating the G$\beta\gamma$ Effects—To examine the functional impact of interaction with G$\beta\gamma$ with NT and CT, we expressed three truncated constructs of α_{1C}: $\Delta C_{1700\text{-end}}$ ("ΔC") which lacks the distal part of the CT; ΔN_{2-139} ("ΔN") missing most of NT; and the double deletion mutant ΔNΔC, missing both pieces. Since it has been shown previously that neither NT nor CT deletions significantly alter the amount of α_{1C} in the plasma membrane (16, 38), we injected the standard amounts of channel RNA to obtain similar levels of channel expression. Wild-type (WT) and truncated α_{1C} were coexpressed with $\alpha_2\delta$, with or without G$\beta\gamma$. Peak I_{Ba} was increased 10-, 22-, and 80-fold by the deletion of the NT, CT, and both termini, respectively (Fig. 3*A*). The current-voltage (I-V) relationship was not significantly affected by each individual deletion, but I-V of ΔNΔC was shifted to the *left* (Fig. 3*B*). Fig. 3*C* shows that all deletions resulted in abolition of the G$\beta\gamma$-induced decrease in I_{Ba} (which was 26.1 ± 3.7% in these three experiments). In all cases, the inhibition was lost and, in $\Delta C_{1700\text{-end}}$ and ΔNΔC, there was even a small enhancement of the current. Thus, both N and C termini are indispensable for the G$\beta\gamma$-induced inhibition.

The Inhibitory Effect of G$\beta\gamma$ is Ca^{2+}- and Calmodulin-dependent—Although Ba^{2+} was used as the charge carrier, we were surprised to find that, in oocytes injected shortly before the experiment with a high-affinity Ca^{2+} chelator, EGTA, the inhibition by coexpressed G$\beta\gamma$ was lost (Fig. 4*A*),

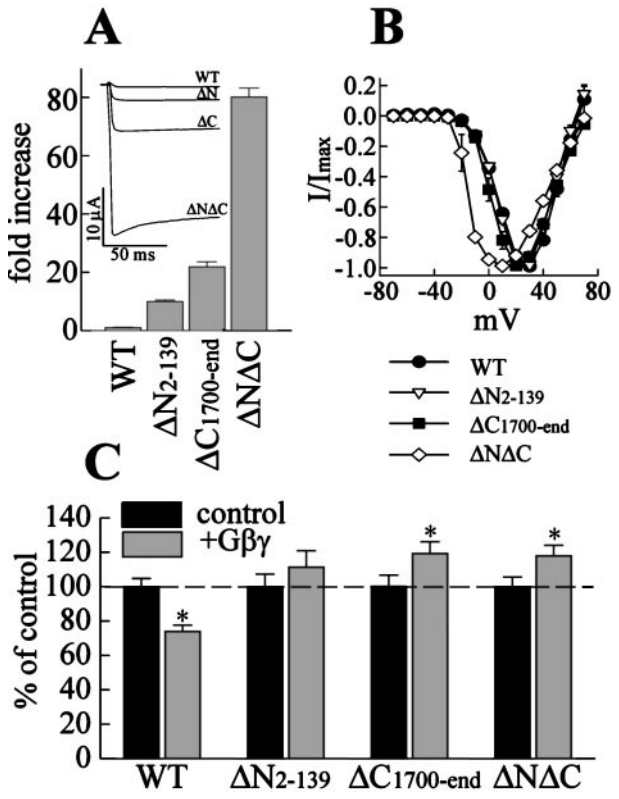

FIG. 3. **Role of N and C termini in the inhibition of α_{1C} by G$\beta\gamma$.** *A,* comparison of the effects of deletions of N and C termini on the amplitude of I_{Ba}. All α_{1C} RNA constructs were injected at the same concentration (2.5 ng/oocyte), with 2.5 ng/oocyte $\alpha_2\delta$ RNA. $n = 6, N = 1$. The *inset* shows Ba^{2+} currents in representative oocytes. I_{Ba} in each oocyte was normalized to the average current in the control group (WT α_{1C}). *B,* current-voltage (I-V) curves of Ba^{2+} currents via channels containing WT and mutant α_{1C} in oocytes of one batch (6 oocytes in each group). In each oocyte, I_{Ba} at all voltages was normalized to the peak current. *C,* wild type α_{1C} (2.5 ng of RNA/oocyte) or its truncated mutants ΔN_{2-139} (0.8 ng of RNA/oocyte), $\Delta C_{1700\text{-end}}$ (0.8 ng of RNA/oocyte), and ΔNΔC (0.2 or 0.4 ng of RNA/oocyte) were coexpressed with $\alpha_2\delta$ (same RNA amounts as α_{1C}), with or without G$\beta\gamma$. In each oocyte, I_{Ba} was normalized to the mean amplitude of I_{Ba} in the control group of oocytes of the same donor, expressing the same α_{1C} variant. The normalized values were averaged across all oocyte batches tested. *, statistically significant differences ($p < 0.05$ or better). Each *bar* represents results from 22 to 29 cells from three batches.

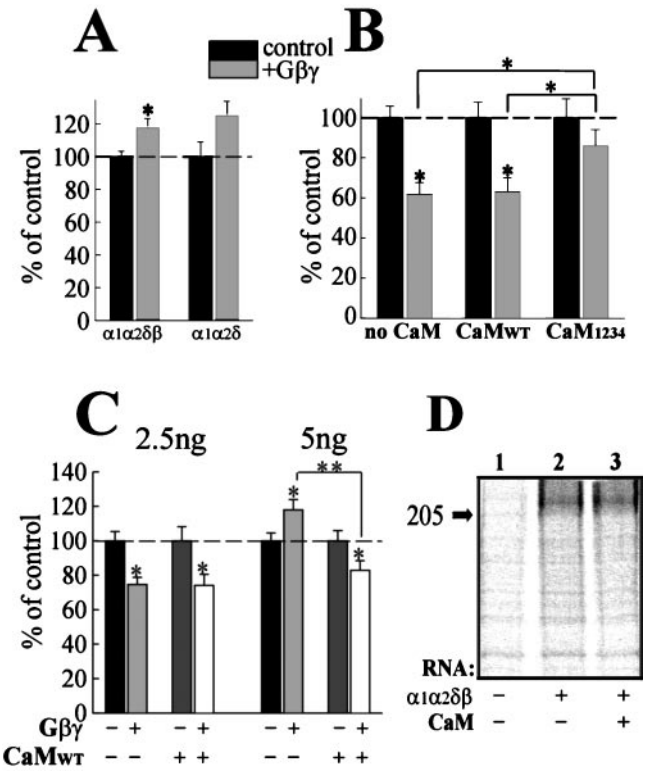

FIG. 4. **The inhibitory effect of G$\beta\gamma$ is Ca^{2+}- and calmodulin-dependent.** *A,* injection of EGTA (50 mM solution, 20 nl/oocyte) abolishes the inhibitory effect of G$\beta\gamma$ and uncovers the G$\beta\gamma$-induced enhancement of I_{Ba}. This effect is observed with L-type channels of the full subunit composition (*left pair of bars*) or of the $\alpha_1\alpha_2\delta$ composition (*right pair of bars*). Each *bar* shows data from 14–26 oocytes (3 batches) normalized as described under "Experimental Procedures." *, statistically significant differences between control and G$\beta\gamma$-expressing groups ($p < 0.05$ or better). *B,* coexpression of the dominant negative mutant of calmodulin, CaM_{1234} (10 ng of RNA/oocyte), but not the WT calmodulin, attenuates the inhibition caused by G$\beta\gamma$. Summary of two experiments; 13 oocytes in each group. *, statistically significant differences between control and G$\beta\gamma$-expressing groups ($p < 0.01$ or better). *C,* coexpression of the WT calmodulin restores the inhibitory effect of G$\beta\gamma$ in oocytes expressing large amounts of L-type channels. Summary of experiments in 3 oocyte batches; each *bar* summarizes results from 20 oocytes. The *left half* of the chart shows the attenuation of I_{Ba} in these 3 batches of oocytes under standard conditions (channel subunits RNAs at 2.5 ng/oocyte; $\alpha_1\alpha_2\delta$ composition), with or without calmodulin. The *right half* of the chart shows the same but at high levels of channel expression, with 5 ng of RNA of each subunit. *, statistically significant differences between control (no G$\beta\gamma$) and G$\beta\gamma$-expressing groups ($p < 0.05$ or better). **, $p < 0.001$. *D,* coexpression of CaM does not alter the amount of α_{1C} protein. CaM_{WT} (10 ng of RNA/oocyte) was coexpressed with the channel (full subunit composition; 1 ng of RNA/oocyte of each subunit). After 4 days of incubation, α_{1C} protein was immunoprecipitated from 5 whole oocytes.

suggesting that the G$\beta\gamma$-induced inhibition requires the presence of a certain basal level of Ca^{2+}. Since G$\beta\gamma$ binding to CT and NT was Ca^{2+}-independent (Fig. 1), it was plausible that a Ca^{2+}-binding protein such as CaM was involved in the G$\beta\gamma$-induced inhibition. To test this idea, we coexpressed the L-type channel with either the wild-type calmodulin, CaM_{WT}, or its dominant negative mutant, Ca^{2+}-insensitive mutant CaM_{1234} (47). Interestingly, expression of CaM itself increased I_{Ba}. At the standard level of channel expression (2.5 ng of RNA/oocyte; $\alpha_1\alpha_2/\delta$ channels), the increase was not significant (22.6 ± 12.7%, $n = 20, N = 3$; $p = 0.12$). However, at the high level of channel expression (5 ng/oocyte) there was a large, highly significant increase in I_{Ba} (63.6 ± 15%; $n = 20, N = 3, p < 0.001$). This is in line with the notion that, at lower channel levels, there is enough endogenous CaM; therefore, the effect of expressed CaM becomes evident only at high levels of expressed channels. Similar results were obtained when CaM RNA was injected 2–3 days after the channels RNA (data not shown). In contrast, CaM_{1234} reduced I_{Ba} by 31 ± 10% ($n = 13$, $N = 2$, $p < 0.05$) at the standard channel concentration.

As shown in Fig. 4*B*, at standard levels of channel expression, CaM_{WT} did not alter the effect of G$\beta\gamma$, while CaM_{1234} significantly attenuated the G$\beta\gamma$-induced inhibition. These results support the assumption that CaM may participate in G$\beta\gamma$-dependent inhibition. It was therefore likely that CaM may be the endogenous factor "missing" for the inhibitory effect of G$\beta\gamma$ when high doses of channel are expressed. To examine this assumption, we coinjected either standard (2.5 ng/oocyte) or high (5 ng/oocyte) doses of RNA of α_1 and $\alpha_2\delta$ subunits, with RNAs of G$\beta\gamma$ and CaM_{WT}. As in the previous experiments, we observed the inhibitory effect of G$\beta\gamma$ on I_{Ba} with the standard RNA concentration (Fig. 4*C, left panel*), and the opposite effect of G$\beta\gamma$ when the channel was expressed at a higher level (Fig. 4*C, right panel*). Coexpression of CaM_{WT} together with G$\beta\gamma$ in the conditions of high level of expression of the channel resulted in a partial restoration of the inhibitory effect of G$\beta\gamma$ (Fig. 4*C, right panel*). None of the effects of CaM coexpression could be attributed to a change in the level of α_{1C} in the oocytes,

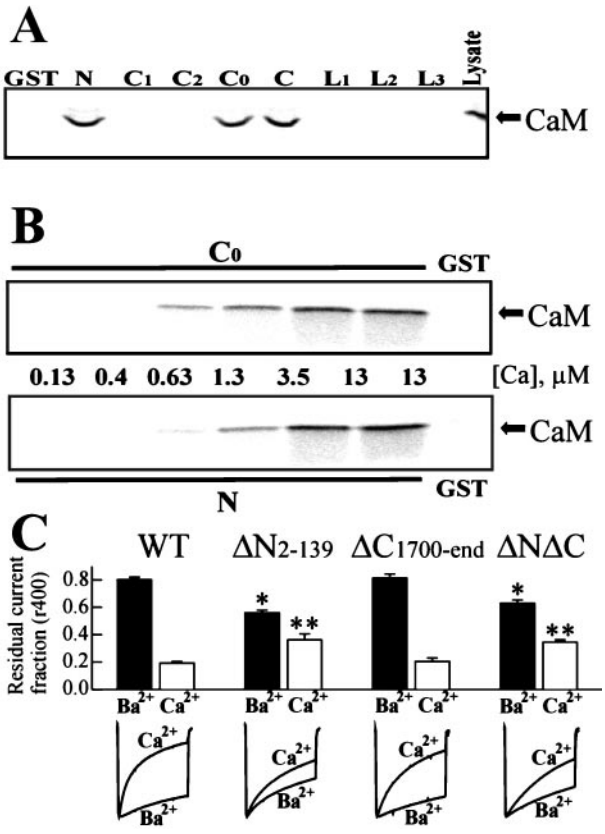

FIG. 5. **CaM binds to NT and CT in a Ca^{2+}-dependent manner.** *A,* binding of ^{35}S-labeled CaM to different fragments of α_{1C}. Immobilized GST fusion proteins were incubated with calmodulin in the presence of 1 mM Ca^{2+}. After washing, calmodulin bound to fusion proteins was eluted and resolved by SDS-PAGE. Identical data were obtained in two more experiments. *B,* CaM binding to N (*lower panel*) and C_0 (*upper panel*) GST fusion proteins at different free Ca^{2+} concentrations (*numbers* are shown between the panels in μM). *C,* Ca^{2+}-dependent inactivation is attenuated by the removal of the NT. Gβγ and/or calmodulin were coexpressed with the channel subunits (α_{1C} + $\alpha_2\delta$ + β_2A; 1 ng/oocyte). Ca^{2+}-dependent inactivation was studied in oocytes injected with 20 nl of 50 mM solution of BAPTA, 10–60 min before measuring the current. Current were monitored in extracellular solutions containing 40 mM Ba^{2+} (WT) or 2 mM Ba^{2+} (other groups), or 40 mM Ca^{2+} (all groups). *Upper panel* shows the summary from two experiments (6–8 oocytes in each group), *lower panel* shows examples of I_{Ba} or I_{Ca} in individual oocytes (currents were scaled to peak amplitudes of I_{Ba} or I_{Ca}). *Single asterisks* (*) show statistically significant differences in r_{400} for I_{Ba} ($p < 0.05$) from the WT group; *double asterisks* (**) show the same but for I_{Ca} (one-way ANOVA was performed separately for I_{Ba} and I_{Ca}).

since the latter remained unchanged, as determined by immunoprecipitation of ^{35}S-labeled α_{1C} from whole oocytes (Fig. 4*D*).

Interaction of Calmodulin with Cytosolic Parts of α_{1C} and the Role of the N Terminus—Fig. 5*A* shows that CaM_{WT} binds *in vitro* to GST fusion proteins of full-length CT and to C_0, the fragment which includes the CaM-binding IQ motif, mapped to the proximal CT (34). We have also identified a novel CaM_{WT}-binding site in the NT (Fig. 5*A*). These interactions were Ca^{2+}-dependent; at 0.1 μM free [Ca^{2+}], no binding of CaM either to NT or CT was observed, and a maximum binding was achieved at about 3 μM (Fig. 5*B*). These results are similar to those previously reported for the CT (34, 36). The CaM_{1234} mutant did not bind to any of the GST fusion proteins neither in the presence nor in the absence of Ca^{2+} (data not shown).

To study the role of the NT and the distal part of the CT in Ca^{2+}-dependent inactivation of I_{Ba}, we used the deletion mutants described above: ΔN_{2-139}, $\Delta C_{1700\text{-end}}$, and ΔNΔC. The decay of Ba^{2+} *versus* Ca^{2+} currents in oocytes injected with BAPTA was compared using the protocol of Peterson *et al.* (37)

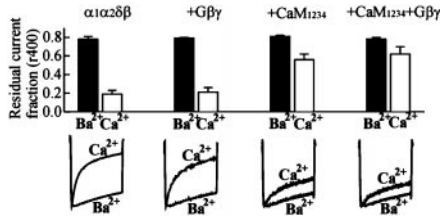

FIG. 6. **Depletion of Gβγ attenuates the Ca^{2+}-dependent inactivation of L-type of Ca^{2+} channel.** Ca^{2+}-dependent inactivation is attenuated by CaM_{1234} but not by the coexpression of Gβγ. Gβγ and/or calmodulin were coexpressed with the channel subunits (α_{1C} + $\alpha_2\delta$ + β_2A; 1 ng/oocyte) as in the previous experiments. The *lower panel* shows representative currents, normalized to peak, for each experimental condition used in this experiment. The *upper panel* shows the mean ± S.E. of all cells tested ($n = 4–5$, $N = 1$).

and Zuhlke *et al.* (36), shown in Fig. 5*C*. The changes in the extent of inactivation were quantitated by measuring the residual current fraction remaining after 400 ms of the depolarizing pulse, r_{400} (36). As expected, with WT α_{1C}, much stronger inactivation was observed in the high-Ca^{2+} than in high-Ba^{2+} solution (Fig. 5*C*). The extent of inactivation with either Ba^{2+} or Ca^{2+} as the charge carrier was not changed in the $\Delta C_{1700\text{-end}}$ mutant, whereas deletion of the NT had profound effects on inactivation. With Ba^{2+}, in the ΔN_{2-139} mutant the inactivation was significantly faster than in WT, whereas the inactivation in the Ca^{2+}-containing solution was weaker than in WT (Fig. 5*C*). The difference between the values of r_{400} in Ba^{2+} and Ca^{2+} was still significant ($p < 0.05$) but greatly reduced as compared with WT. The double deletion mutant ΔNΔC behaved like ΔN_{2-139}. Thus, the acceleration of L-type channel inactivation by Ca^{2+} was severely compromised by the deletion of the NT but not of the distal portion of CT.

To study whether Gβγ affects the Ca^{2+}/CaM-dependent inactivation, we utilized the CaM_{1234} mutant. When expressed in the oocytes, CaM_{1234} suppresses the Ca^{2+}-dependent L-type channel inactivation, presumably by replacing the endogenous CaM_{WT} (36, 37) (see Fig. 6). However, the Ca^{2+}-dependent inactivation remained unaffected by coexpression of Gβγ, either in the absence or presence of CaM_{1234}. The inactivation of Ba^{2+} currents was not affected by either Gβγ or CaM_{1234} (Fig. 6). Thus, coexpressed Gβγ did not affect the inactivation process.

DISCUSSION

This work urges to reconsider the view that L-type Ca^{2+} channels lack interaction with Gβγ and also provides new insights into the mechanisms of L-type channel gating and its modulation by calmodulin. We demonstrate that NT and CT of α_{1C} are partially independent, interacting inhibitory gates. Gβγ directly binds to NT and CT. Coexpression of Gβγ reduces the L-type Ca^{2+} channel currents; this inhibition requires the presence of CaM. CaM binds to CT and to a novel site in NT, which plays an important role in Ca^{2+}/CaM-dependent inactivation.

Interaction of the α_{1C} Subunit of the L-type Channel with Gβγ Affects the Channels Function—Using GST fusion proteins of cytosolic segments of α_{1C}, we demonstrate that Gβγ binds to the NT and to two separate sites in the CT of α_{1C}. The strongest interaction is in the first half of the CT and is probably confined to the first quarter of the CT. The NT shows weaker but also substantial Gβγ binding. In agreement with previous reports (15, 26, 27), the L_1 loop of α_{1C} does not bind Gβγ, and no substantial binding is seen in other intersegment linker loops. Some isoforms of neuronal α_{1C} have a shorter N terminus than the cardiac-type α_{1C} used here (62). However, α_{1C} with a full-length N terminus is also abundant in the brain, at least in rat

(17). Therefore, the present results are relevant both to cardiac and neuronal L-type Ca^{2+} channels.

The electrophysiological experiments in *Xenopus* oocytes showed that coexpression of G$\beta\gamma$ caused a reduction of the whole cell the Ca^{2+} channel current. This phenomenon was in the focus of this study. This inhibition was not due to a decrease in the amount of channel protein. This was shown by direct immunochemical measurements and by demonstrating that expression of G$\beta\gamma$ still reduced I_{Ba} at a time when the number of the functional channels had reached a steady level. Thus, the inhibition caused by coexpression of G$\beta\gamma$ reflected a change in the function of the L-type channels. Both NT and CT were indispensable for this inhibition, which was lost after deletion of either NT or CT. The disappearance of G$\beta\gamma$-induced inhibition could not be due to an increase in the level of α_{1C} protein by one of the deletions, since removal of either NT or $CT_{1700\text{-end}}$ does not increase the amount of α_{1C} in the oocytes plasma membrane (16, 17, 38).

Under conditions that weakened the inhibitory effect of G$\beta\gamma$ (EGTA, high levels of channel expression, NT and CT deletions), we often observed a small enhancement of I_{Ba}. This phenomenon was much less pronounced and has been less well characterized. It could be due to a small increase in the amount of α_{1C} observed upon coexpression of G$\beta\gamma$ (Fig. 2*E*).

Presumably, overexpression of G$\beta\gamma$ may cause general changes in the metabolic state of the cell and activate various signal transduction pathways, causing permanent changes in Ca^{2+} channels state. At present we cannot exclude the possibility that these phenomena might contribute to the observed effects of G$\beta\gamma$. However, the findings that the inhibition was removed acutely after EGTA injection, and by the deletion of G$\beta\gamma$-binding elements, especially the NT, argue in favor of a more direct effect of G$\beta\gamma$.

Possible Role of G$\beta\gamma$ Modulation of the L-Type Ca^{2+} Channel—Although our results do not explicitly assign a physiological role for the observed effects of G$\beta\gamma$ discovered here, several possibilities can be proposed. The most exciting one is that the direct interaction of G$\beta\gamma$ with α_{1C} plays a role in mediating the inhibitory effects of G protein-coupled neurotransmitters on L-type channels. Neuronal L-type Ca^{2+} channels are inhibited by neurotransmitters acting via G proteins of the G_q class through an unidentified second messenger (see Ref. 63), and also via pertussis toxin-sensitive $G_{i/o}$ proteins (*e.g.* Refs. 60, 64, and 65). All these effects are voltage-independent. Although specific Gβ subunits have been shown to be indispensable for $G_{i/o}$-mediated inhibitions (56), the details of the pathway(s) that involve this class of G proteins remain unknown. Even in cardiac cells, where the inhibitory effect of acetylcholine of L-type Ca^{2+} channel has been extensively studied (8, 9), the mechanism of inhibition of basal I_{Ca} by ACh (in the absence of stimulation of adenylyl cyclase) is not fully understood (*e.g.* Ref. 66). Our and others' (32, 40, 41, 67) inability to reconstitute neurotransmitter-induced inhibition of L-type I_{Ca} in heterologous expression systems precluded the study of the mechanism of such inhibition. We stress that failure to obtain such reconstitution does not argue against either membrane delimited or second messenger-mediated mechanism. It simply suggests that an additional unknown component (*e.g.* a protein), present in neurons and heart, is missing in the oocytes and HEK cells (as is partially supported by our preliminary data concerning coexpression of $G\alpha_o$). In a "normal" cell, this missing element may be needed, for example, to anchor G$\beta\gamma$ near α_{1C}; overexpression of G$\beta\gamma$ as done in our experiments is expected to increase the local concentration of G$\beta\gamma$ near the channel, partially alleviating the need for the anchor.

An alternative explanation for the discrepancy between the inhibition of L-type Ca^{2+} channel by overexpression of G$\beta\gamma$ *versus* the absence of effects of neurotransmitters is that, indeed, there is no "fast" modulation by G$\beta\gamma$ released from G$\alpha\beta\gamma$ heterotrimers. If this is the case, the direct G$\beta\gamma$-α1C interaction still may be an important regulator on a long time scale, whereby the function of the L-type channel may be altered by long-term changes in G$\beta\gamma$ concentration or its subcellular localization.

The Role of Ca^{2+} and CaM in Regulation of L-type Channel by $G_{\beta\gamma}$—The inhibition by G$\beta\gamma$ appeared to be Ca^{2+}-dependent, since it was eliminated by intracellular Ca^{2+} buffering with EGTA, although not by BAPTA (data not shown). On the other hand, G$\beta\gamma$ inhibition did not require Ca^{2+} entry (Ba^{2+} currents were monitored), suggesting that a basal cellular level of Ca^{2+} is sufficient. BAPTA, a faster chelator than EGTA but of lower affinity for Ca^{2+} (68), may not be as efficient as EGTA in reducing the basal Ca^{2+} levels under the conditions used here (about 1 mM EGTA or BAPTA in the cytosol). An alternative possibility of a Ca^{2+}-independent "pharmacological" effect of EGTA cannot be discounted at present.

Several lines of evidence suggested that an oocyte's endogenous calmodulin is needed for the inhibitory effect of G$\beta\gamma$: (i) the G$\beta\gamma$-induced inhibition disappeared at high levels of channel expression, suggesting that an endogenous protein that normally regulates the channel is in short supply; (ii) coexpression of CaM restored the inhibitory effect of G$\beta\gamma$ at high levels of channel expression; and (iii) the inhibitory effect of G$\beta\gamma$ was strongly attenuated by the negative dominant CaM mutant, CaM_{1234}, which misses all four Ca^{2+}-binding sites (47).

CaM is an extremely important regulator of Ca^{2+} and other ion channels (69), and our results provide new insights into the mechanisms of its action. We find that, in addition to the previously identified C-terminal CaM-binding site in α_{1C} (containing the IQ domain, aa 1655–1665 (34, 37)), CaM also binds to the NT. Deletion of NT greatly attenuates the Ca^{2+}-dependent inactivation, supporting an important role for this CaM-binding site.

G$\beta\gamma$ appears to affect CaM action on the L-type Ca^{2+} channel. Since expression of G$\beta\gamma$ does not affect the Ca^{2+}/CaM-dependent inactivation (see Fig. 6), it is unlikely that G$\beta\gamma$ interferes with this process. The facilitating effect of CaM is less obvious than inactivation in the oocyte system, but we propose that facilitation is reflected in the increase in I_{Ba} caused by coexpression of CaM. This effect was observed under "resting" conditions (no Ca^{2+} influx, no coexpressed G$\beta\gamma$). In support of this hypothesis, the anti-CaM treatment by CaM_{1234} decreased I_{Ba}. Furthermore, coexpression of CaM increased I_{Ba} at high levels of channel expression, when the endogenous CaM might be in short supply, but only marginally affected the channel at low expression levels (when the endogenous CaM is sufficient). These data suggest that, under resting conditions, CaM constitutively facilitates the function of the Ca^{2+} channel. The inhibition by G$\beta\gamma$ would then oppose this facilitating effect of CaM, explaining the Ca^{2+}/CaM and expression level dependence of G$\beta\gamma$ modulation. There are precedents for opposing interactions between CaM and G$\beta\gamma$: G$\beta\gamma$ binding to CaM prevents the formation of G$\alpha\beta\gamma$ heterotrimers (70); G$\beta\gamma$ and CaM oppositely regulate certain types of adenylyl cyclases (71); CaM promotes dissociation of bound G$\beta\gamma$ from a glutamatergic metabotropic receptor (72).

Several questions remain open. First, the affinity of free CaM for Ca^{2+} (K_d of about 10 μM; see Ref. 73) is too low to support the G$\beta\gamma$ inhibition, which occurs at basal cellular levels of Ca^{2+} (probably close to 0.1 μM). However, the presence of CaM effectors (α_{1C} and/or G$\beta\gamma$ in our case) is known to increase the affinity of Ca^{2+}/CaM interaction (73). Although CaM does

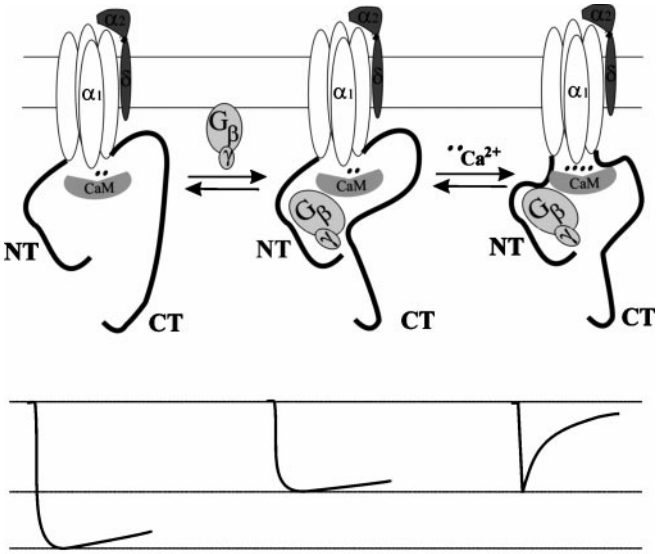

FIG. 7. **Schematic representation of the NT/CT scaffold model.** A cartoon of channel states is shown at the *top*; corresponding Ba^{2+} or Ca^{2+} currents are drawn at the *bottom*. In the resting state, at basal cellular Ca^{2+} levels, NT and CT are loosely folded; CaM may be anchored with only a fraction of its Ca^{2+}-binding sites occupied by Ca^{2+}; depolarization causes large, poorly inactivating currents in a high-Ba^{2+}, Ca^{2+}-free solution (*left*). Binding of G$\beta\gamma$ causes tightening of the scaffold and a decrease in the current (*middle*). A switch to a Ca^{2+}-containing solution and the entry of Ca^{2+} causes a forceful tightening of the scaffold and inactivation, due to strong binding of CaM to its NT- and CT-binding sites; this process is largely unaffected by G$\beta\gamma$.

not interact with GST fusion proteins of either NT or CT at basal Ca^{2+} levels (Fig. 5), higher affinity may be envisioned within a hypothetical binding site formed jointly by NT and CT (see below). Thus, theoretically, basal Ca^{2+} levels may suffice to support CaM-α_{1C} interaction and thus G$\beta\gamma$ inhibition, but this point requires further clarification. Second, CaM is an abundant cellular protein. It seems surprising that there is not enough for the modulation of Ca^{2+} channels when they are expressed at relatively high levels. However, most of the cellular CaM may not be free but pre-assembled with its other effectors.

Role of N and C Termini in L-type Ca^{2+} Channel Gating: an NT/CT Scaffold Model—In L-type Ca^{2+} channels, NT and CT appear to act as inhibitory gates that attenuate the channels activation by depolarization; their removal increases the ionic currents without an increase in expression levels (16, 38, 39). Joint removal of both NT and $CT_{1700\text{-end}}$ (in the $\Delta N\Delta C$ mutant), performed here for the first time, revealed an even greater increase in the macroscopic I_{Ba} than the removal of each terminus separately. Peak I_{Ba} was increased ~10-fold by the deletion of the NT, ~22-fold by the deletion of the $CT_{1700\text{-end}}$, and ~80-fold by the deletion of both (Fig. 3). Thus, each inhibitory gate (NT and CT) has an inhibitory effect of its own, and neither one is permissive for the other, otherwise the removal of either one would already have caused a maximal effect.

On the other hand, the maximal effect of the joint removal of two independent gates would be a multiple of the individual effects, *i.e.* a 220-fold increase in I_{Ba} (the open probability of a single $\alpha_1\alpha_2\delta$ channel is below 0.0005 (52), and such a change is theoretically possible). Furthermore, the current-voltage curve was not significantly affected by either CT or NT deletion (16, 38, 39), but was shifted to the left by deletion of both termini (Fig. 3), suggesting their synergistic effect on activation gating. Finally, both NT and CT were indispensable for the G$\beta\gamma$-induced inhibition: removal of either terminus eliminated the inhibition. Therefore, we conclude that CT and NT are interacting gates. Importantly, the major G$\beta\gamma$-binding site of the CT is located before aa 1700. The fact that the deletion of the CT beyond aa 1700 fully eliminates the G$\beta\gamma$ effect implies that it is the removal of the gating element, rather than of the G$\beta\gamma$-binding site, which causes this effect. (Alternatively, it may suggest a great functional importance for the weak G$\beta\gamma$-binding site found in the second half of CT.)

Based on these considerations, we propose that C and N termini act as partially independent but interacting gates that form a molecular scaffold at the cytoplasmic side of the channel, which deters channel opening, probably by an allosteric mechanism. Its conformation changes as a function of the presence of Ca^{2+} and of the extent of interaction between G$\beta\gamma$ and CaM; other cytosolic parts of α_{1C} and the Ca^{2+} channel β subunit may contribute to scaffolds formation. We propose that factors that "tighten" the interaction between NT and CT strengthen the inhibitory control exerted by the scaffold. Fig. 7 presents a simplified scheme of this model and of the way G$\beta\gamma$ and CaM regulate gating. The scaffold harbors at least two binding sites for each CaM and G$\beta\gamma$, in each of the termini. G$\beta\gamma$ binds to the scaffold in the absence of elevated Ca^{2+} and reduces the current by strengthening the interaction between CT and NT and/or by opposing a "basal" facilitating effect of CaM. Influx of Ca^{2+} via the open channel is followed by Ca^{2+} binding to CaM which, in turn, improves the interaction of CaM with its binding sites and further tightens the scaffold, causing more inhibition (which is apparent as Ca^{2+}-dependent inactivation). The latter effect is G$\beta\gamma$-independent.

This model actually presents a further elaboration of that proposed by Peterson *et al.* (37) to explain Ca^{2+}-dependent inactivation. It has been envisaged that CaM, which in the absence of Ca^{2+} must be tethered to a site distinct from the C-terminal IQ domain, binds to the latter following Ca^{2+} influx and binding. Together with the yet undefined tethering element, the CT has been proposed to form a scaffold which, after binding of Ca^{2+}/CaM, induces inactivation. The necessity for a CaM tethering element that should bind CaM in the absence of Ca^{2+} was also stressed by Qin *et al.* (34) and Zuhlke *et al.* (36). However, although we have tested the binding of CaM to all large cytosolic parts of α_{1C}, no Ca^{2+}-independent binding sites could be found. Furthermore, the CaM_{1234} mutant, which is supposed to act by replacing the endogenous WT CaM at the tethering site, did not bind to any of our GST fusion proteins either in the absence or presence of Ca^{2+}. Possibly, the three-dimensional structure of the N/C-terminal scaffold is such that the NT and CT CaM-binding sites actually form one, high-affinity site which may anchor CaM (or CaM_{1234}) in the absence of elevated Ca^{2+} (alternatively, the small linkers within the homology domains may contribute to the anchoring site). A high-affinity site for G$\beta\gamma$ may also be jointly formed by the three sites (NT, proximal CT, distal CT) identified here, eventually providing for a 1:1 stoichiometry for G$\beta\gamma$ binding (as appears to be the case with α_{1B}; see Ref. 25).

Acknowledgments—We thank Ilana Lotan and Dafna Singer-Lahat for helpful comments and critical reading of the manuscript, and Daniel Chananashvili for advice.

REFERENCES

1. Hille, B. (1992) *Ionic Channels of Excitable Membranes*, Sinauer, Sunderland
2. Snutch, T. P., and Reiner, P. B. (1992) *Curr. Opin. Neurobiol.* **2,** 247–253
3. Catterall, W. A. (1998) *Cell Calcium* **24,** 307–323
4. Perez-Reyes, E. (1998) *J. Bioenerg. Biomembr.* **30,** 313–318
5. Reuter, H. (1983) *Nature* **301,** 569–574
6. Finkbeiner, S., and Greenberg, M. E. (1998) *J. Neurobiol.* **37,** 171–189
7. Armstrong, C. M., and Hille, B. (1998) *Neuron* **20,** 371–380
8. Trautwein, W., and Hescheler, J. (1990) *Annu. Rev. Physiol.* **52,** 257–274
9. Wickman, K., and Clapham, D. E. (1995) *Physiol. Rev.* **75,** 865–885
10. Hosey, M., Chien, A. J., and Puri, T. S. (1996) *Trends Cardiovasc. Med.* **6,** 265–273
11. Zamponi, G. W., and Snutch, T. P. (1998) *Curr. Opin. Neurobiol.* **8,** 351–356

12. Dolphin, A. C. (1998) *J. Physiol.* (*Lond.*) **506,** 3–11
13. Ikeda, S. R., and Dunlap, K. (1999) *Adv. Second Messenger Phosphoprotein Res.* **33,** 131–151
14. Fraser, I. D. C., and Scott, J. D. (1999) *Neuron* **23,** 423–426
15. Zamponi, G. W., Bourinet, E., Nelson, D., Nargeot, J., and Snutch, T. P. (1997) *Nature* **385,** 442–446
16. Shistik, E., Ivanina, T., Blumenstein, Y., and Dascal, N. (1998) *J. Biol. Chem.* **273,** 17901–17909
17. Shistik, E., Keren-Raifman, T., Idelson, G. H., Dascal, N., and Ivanina, T. (1999) *J. Biol. Chem.* **274,** 31145–31149
18. Gao, T., Yatani, A., Dell'Acqua, M. L., Sako, H., Green, S. A., Dascal, N., Scott, J. D., and Hosey, M. M. (1997) *Neuron* **19,** 185–196
19. Bunemann, M., Gerhardstein, B. L., Gao, T., and Hosey, M. M. (1999) *J. Biol. Chem.* **274,** 33851–33854
20. Bernheim, L., Beech, D. J., and Hille, B. (1991) *Neuron* **6,** 859–867
21. Diverse-Pierluissi, M., and Dunlap, K. (1993) *Neuron* **10,** 753–760
22. Diverse-Pierluissi, M., Goldsmith, P. K., and Dunlap, K. (1995) *Neuron* **14,** 191–200
23. Shapiro, M. S., Wollmuth, L. P., and Hille, B. (1994) *J. Neurosci.* **14,** 7109–7116
24. Patil, P. G., de Leon, M., Reed, R. R., Dubel, S., Snutch, T. P., and Yue, D. T. (1996) *Biophys. J.* **71,** 2509–2521
25. Zamponi, G. W., and Snutch, T. P. (1998) *Proc. Natl. Acad. Sci. U. S. A.* **95,** 4035–4039
26. De Waard, M., Liu, H., Walker, D., Scott, V. E., Gurnett, C. A., and Campbell, K. P. (1997) *Nature* **385,** 446–450
27. Qin, N., Platano, D., Olcese, R., Stefani, E., and Birnbaumer, L. (1997) *Proc. Natl. Acad. Sci. U. S. A.* **94,** 8866–8871
28. Page, K. M., Canti, C., Stephens, G. J., Berrow, N. S., and Dolphin, A. C. (1998) *J. Neurosci.* **18,** 4815–4824
29. Canti, C., Page, K. M., Stephens, G. J., and Dolphin, A. C. (1999) *J. Neurosci.* **19,** 6855–6864
30. Simen, A. A., and Miller, R. J. (1998) *J. Neurosci.* **18,** 3689–3698
31. Furukawa, T., Nukada, T., Mori, Y., Wakamori, M., Fujita, Y., Ishida, H., Fukuda, K., Kato, S., and Yoshii, M. (1998) *J. Biol. Chem.* **273,** 17585–17594
32. Herlitze, S., Hockerman, G. H., Scheuer, T., and Catterall, W. A. (1997) *Proc. Natl. Acad. Sci. U. S. A.* **94,** 1512–1516
33. Eckert, R., and Chad, J. E. (1984) *Prog. Biophys. Mol. Biol.* **44,** 215–267
34. Qin, N., Olcese, R., Bransby, M., Lin, T., and Birnbaumer, L. (1999) *Proc. Natl. Acad. Sci. U. S. A.* **96,** 2435–2438
35. Lee, A., Wong, S. T., Gallagher, D., Li, B., Storm, D. R., Scheuer, T., and Catterall, W. A. (1999) *Nature* **399,** 155–159
36. Zuhlke, R. D., Pitt, G. S., Deisseroth, K., Tsien, R. W., and Reuter, H. (1999) *Nature* **399,** 159–162
37. Peterson, B. Z., DeMaria, C. D., Adelman, J. P., and Yue, D. T. (1999) *Neuron* **22,** 549–558
38. Wei, X., Neely, A., Lacerda, A. E., Olcese, R., Stefani, E., Perez-Reyes, E., and Birnbaumer, L. (1994) *J. Biol. Chem.* **269,** 1635–1640
39. Klockner, U., Mikala, G., Varadi, M., Varadi, G., and Schwartz, A. (1995) *J. Biol. Chem.* **270,** 17306–17310
40. Bourinet, E., Charnet, P., Tomlinson, W. J., Stea, A., Snutch, T. P., and Nargeot, J. (1994) *EMBO J.* **13,** 5032–5039
41. Bourinet, E., Soong, T. W., Stea, A., and Snutch, T. P. (1996) *Proc. Natl. Acad. Sci. U. S. A.* **93,** 1486–1491
42. Zhang, J. F., Ellinor, P. T., Aldrich, R. W., and Tsien, R. W. (1996) *Neuron* **17,** 991–1003
43. Sculptoreanu, A., Rotman, E., Takahashi, M., Scheuer, T., and Catterall, W. A. (1993) *Proc. Natl. Acad. Sci. U. S. A.* **90,** 10135–10139
44. Dai, S., Klugbauer, N., Zong, X., Seisenberger, C., and Hofmann, F. (1999) *FEBS Lett.* **442,** 70–74
45. Liman, E. R., Tytgat, J., and Hess, P. (1992) *Neuron* **9,** 861–871
46. Jing, J., Chikvashvili, D., Singer-Lahat, D., Thornhill, W. B., Reuveny, E., and Lotan, I. (1999) *EMBO J.* **18,** 1245–1256
47. Xia, X. M., Fakler, B., Rivard, A., Wayman, G., Johnson-Pais, T., Keen, J. E., Ishii, T., Hirschberg, B., Bond, C. T., Lutsenko, S., Maylie, J., and Adelman, J. P. (1998) *Nature* **395,** 503–507
48. Singer, D., Biel, M., Lotan, I., Flockerzi, V., Hofmann, F., and Dascal, N. (1991) *Science* **253,** 1553–1557
49. Mikami, A., Imoto, K., Tanabe, T., Niidome, T., Mori, Y., Takeshima, H., Narumiya, S., and Numa, S. (1989) *Nature* **340,** 230–233
50. Dascal, N., and Lotan, I. (1992) in *Protocols in Molecular Neurobiology* (Longstaff, A., and Revest, P., eds) Vol. 13, pp. 205–225, Humana Press, Totowa, NJ
51. Ivanina, T., Perets, T., Thornhill, W. B., Levin, G., Dascal, N., and Lotan, I. (1994) *Biochemistry* **33,** 8786–8792
52. Shistik, E., Ivanina, T., Puri, T., Hosey, M., and Dascal, N. (1995) *J. Physiol.* (*Lond.*) **489,** 55–62
53. Chien, A. J., Zhao, X., Shirokov, R. E., Puri, T. S., Chang, C. F., Sun, D., Rios, E., and Hosey, M. M. (1995) *J. Biol. Chem.* **270,** 30036–30044
54. Sharon, D., Vorobiov, D., and Dascal, N. (1997) *J. Gen. Physiol.* **109,** 477–490
55. Clapham, D. E., and Neer, E. J. (1997) *Annu. Rev. Pharmacol. Toxicol.* **37,** 167–203
56. Kleuss, C., Scherubl, H., Hescheler, J., Schultz, G., and Wittig, B. (1992) *Nature* **358,** 424–426
57. Hescheler, J., and Schultz, G. (1994) *Ann. N. Y. Acad. Sci.* **733,** 306–312
58. Garcia, D. E., Li, B., Garcia-Ferreiro, R. E., Hernandez-Ochoa, E. O., Yan, K., Gautam, N., Catterall, W. A., Mackie, K., and Hille, B. (1998) *J. Neurosci.* **18,** 9163–9170
59. Ruiz-Velasco, V., and Ikeda, S. R. (2000) *J. Neurosci.* **20,** 2183–2191
60. Kleuss, C., Hescheler, J., Ewel, C., Rosenthal, W., Schultz, G., and Wittig, B. (1991) *Nature* **353,** 43–48
61. Dascal, N., Doupnik, C. A., Ivanina, T., Bausch, S., Wang, W., Lin, C., Garvey, J., Chavkin, C., Lester, H. A., and Davidson, N. (1995) *Proc. Natl. Acad. Sci. U. S. A.* **92,** 6758–6762
62. Snutch, T. P., Tomlinson, W. J., Leonard, J. P., and Gilbert, M. M. (1991) *Neuron* **7,** 45–57
63. Shapiro, M. S., Loose, M. D., Hamilton, S. E., Nathanson, N. M., Gomeza, J., Wess, J., and Hille, B. (1999) *Proc. Natl. Acad. Sci. U. S. A.* **96,** 10899–10904
64. Rosenthal, W., Hescheler, J., Hinsch, K. D., Spicher, K., Trautwein, W., and Schultz, G. (1988) *EMBO J.* **7,** 1627–1633
65. Akopian, A., Johnson, J., Gabriel, R., Brecha, N., and Witkovsky, P. (2000) *J. Neurosci.* **20,** 929–936
66. Ye, C., Sowell, M. O., Vassilev, P. M., Milstone, D. S., and Mortensen, R. M. (1999) *J. Mol. Cell Cardiol.* **31,** 1771–1781
67. Furukawa, T., Miura, R., Mori, Y., Strobeck, M., Suzuki, K., Ogihara, Y., Asano, T., Morishita, R., Hashii, M., Higashida, H., Yoshii, M., and Nukada, T. (1998) *J. Biol. Chem.* **273,** 17595–17603
68. Tsien, R. Y. (1980) *Biochemistry* **19,** 2396–2404
69. Levitan, I. B. (1999) *Neuron* **22,** 645–648
70. Liu, M., Yu, B., Nakanishi, O., Wieland, T., and Simon, M. (1997) *J. Biol. Chem.* **272,** 18801–18807
71. Sunahara, R. K., Dessauer, C. W., and Gilman, A. G. (1996) *Annu. Rev. Pharmacol. Toxicol.* **36,** 461–480
72. O'Connor, V., El Far, O., Bofill-Cardona, E., Nanoff, C., Freissmuth, M., Karschin, A., Airas, J. M., Betz, H., and Boehm, S. (1999) *Science* **286,** 1180–1184
73. Jurado, L. A., Chockalingam, P. S., and Jarrett, H. W. (1999) *Physiol. Rev.* **79,** 661–682